MAJOR ARTICLE

Genetic Switch to Hypervirulence Reduces Colonization Phenotypes of the Globally Disseminated Group A *Streptococcus* M1T1 Clone

Andrew Hollands,[1,3] Morgan A. Pence,[3] Anjuli M. Timmer,[3] Sarah R. Osvath,[2] Lynne Turnbull,[2] Cynthia B. Whitchurch,[2] Mark J. Walker,[1] and Victor Nizet[3,4,5]

[1]School of Biological Sciences, University of Wollongong, Wollongong, and [2]Institute for the Biotechnology of Infectious Diseases, University of Technology, Sydney, New South Wales, Australia; [3]Department of Pediatrics and [4]Skaggs School of Pharmacy and Pharmaceutical Sciences, University of California, San Diego, La Jolla, and [5]Rady Children's Hospital, San Diego, California

Background. The recent resurgence of invasive group A streptococcal disease has been paralleled by the emergence of the M1T1 clone. Recently, invasive disease initiation has been linked to mutations in the *covR/S* 2-component regulator. We investigated whether a fitness cost is associated with the *covS* mutation that counterbalances hypervirulence.

Methods. Wild-type M1T1 group A *Streptococcus* and an isogenic *covS*-mutant strain derived from animal passage were compared for adherence to human laryngeal epithelial cells, human keratinocytes, or fibronectin; biofilm formation; and binding to intact mouse skin. Targeted mutagenesis of capsule expression of both strains was performed for analysis of its unique contribution to the observed phenotypes.

Results. The *covS*-mutant bacteria showed reduced capacity to bind to epithelial cell layers as a consequence of increased capsule expression. The *covS*-mutant strain also had reduced capacity to bind fibronectin and to form biofilms on plastic and epithelial cell layers. A defect in skin adherence of the *covS*-mutant strain was demonstrated in a murine model.

Conclusion. Reduced colonization capacity provides a potential explanation for why the *covS* mutation, which confers hypervirulence, has not become fixed in the globally disseminated M1T1 group A *Streptococcus* clone, but rather may arise anew under innate immune selection in individual patients.

Streptococcus pyogenes (group A *Streptococcus* [GAS]) is a gram-positive, human-specific pathogen responsible for over 500,000 deaths each year worldwide [1]. A resurgence of severe GAS disease in recent decades has been paralleled by the emergence of a globally disseminated GAS clone that belongs to serotype M1T1 [2–4]. M1T1 GAS are the most common cause of streptococcal pharyngitis in developed countries and are strongly overrepresented in cases of severe infection such as necrotizing fasciitis and toxic shock syndrome [5–7].

An inverse relationship exists between the expression of a broad-spectrum secreted cysteine protease, SpeB, and clinical disease severity in clinical isolates of M1T1 GAS [8]. Recently, mutations in the 2-component regulatory system *covR/S* that are characteristic of bloodstream isolates of M1T1 GAS (as opposed to pharyngeal isolates) have been identified [9]. These mutations arise in vivo in the murine model of M1T1 GAS necrotizing fasciitis and lead to loss of SpeB expression and increased virulence [9–12]. SpeB is initially produced as a 40-kDa zymogen, which is then converted to the 28-kDa active form by autocatalytic processing [13]. The role played by SpeB in GAS infection is complex, multifaceted, and incompletely understood. SpeB has been shown to cleave a broad range of host proteins, in-

Received 8 August 2009; accepted 21 January 2010; electronically published 27 May 2010.

Potential conflicts of interest: none reported.

Financial support: National Institutes of Health (grant AI077780 to V.N. and M.J.W.); National Health and Medical Research Council of Australia (grant 459103 to M.J.W. and Senior Research Fellowship to C.B.W.); University of California, San Diego (Neuroscience Microscopy Shared Facility grant P30 NS047101 and Genetics Training Program grant T32 GM008666 to M.A.P.); Australian Government (Australian Postgraduate Award to A.H.); A.P. Giannini Foundation (Postdoctoral Fellowship to A.M.T.).

Reprints or correspondence: Dr Victor Nizet, Division of Pediatric Pharmacology and Drug Discovery, University of California, San Diego, 9500 Gilman Dr, Mail Code 0687, La Jolla, CA 92093 (vnizet@ucsd.edu).

The Journal of Infectious Diseases 2010; 202(1):000–000

0022-1899/2010/20201-00XX$15.00
DOI: 10.1086/653124

cluding components of the extracellular matrix, cytokine precursors, immunoglobulins, and antimicrobial peptides [14–16], which could promote tissue damage or impair host immune functions. However, SpeB also cleaves some of the protein virulence factors of the bacterium, such as the fibrinogen-binding M1 protein [12, 17–19], various superantigens [20, 21], the secreted plasminogen activator streptokinase [22], and the deoxyribonuclease Sda1 [20], which thus attenuates key aspects of GAS pathogenicity.

CovR/S is an important global gene regulator that is responsible for regulating ~10% of the GAS genome [4, 9]. It has been found that CovR acts mainly as a negative regulator, even in the absence of CovS, and that CovS inactivates the function of CovR [23]. Specific point mutations in *covR/S* and truncation mutations in *covS* result in considerable down-regulation of SpeB expression but concurrent up-regulation of many virulence factor genes, including those encoding Sda1, interleukin 8 protease SpyCEP, streptolysin O, streptococcal inhibitor of complement, and the hyaluronic acid capsule synthesis operon [9–12]. It has been hypothesized that increased expression of these virulence determinants, along with sparing them from SpeB degradation, promotes the proliferation and invasive spread of the *covR/S*-mutant strain [9, 10, 24]. Increased resistance to innate immune clearance, and in particular killing by neutrophils, may represent the major selection pressure that favors the *covR/S* mutation in vivo [10].

The routine occurrence of the *covR/S* mutation in M1T1 GAS and the dramatically increased animal virulence that follows this event raise the question of why this particular mutation has not become fixed during GAS evolution. We hypothesized that a counterbalancing selection pressure acts to maintain the wild-type genotype, and thus we sought to elucidate the fitness cost or costs of the *covR/S* mutation in the M1T1 GAS population.

METHODS

Bacterial strains, medium, and growth conditions. Well-characterized M1T1 clinical isolate 5448 and its mouse-passaged *covS*-mutant derivative 5448AP were used [10]. Correction of the *covS* mutation in the 5448AP strain restores wild-type phenotypes [25]. GAS strains were propagated using Todd-Hewitt broth (THB) or Todd-Hewitt agar (THA). *Escherichia coli* were grown using Luria-Bertani broth or Luria-Bertani agar. Erythromycin selection was used at 5 μg/mL for GAS and at 500 μg/mL for *E. coli.*

Growth curves and chain length assays. Overnight cultures of GAS bacteria were diluted into fresh THB, and the optical density at 600 nm (OD_{600}) was measured every 30 min to determine the growth curves. For chain length assays, GAS were centrifuged for 5 min at 3200 *g* to create a monolayer and viewed at 10^{-3} dilution by use of a Zeiss Axiovert 100 inverted microscope, and the chain length was calculated using 1 random field of view from 3 separate wells. Statistical significance was determined using 1-way analysis of variance (ANOVA) with the Tukey post hoc test.

Plasmid integrational mutagenesis. An intragenic fragment of *hasA* was amplified using forward primer *hasA*int-F-*Bam*HI (5′-GCAGGATCCTTGGAACATCAACTGTAGG-3′) and reverse primer *hasA*int-R-*Xba*I (5′-GCATCTAGATTAATTCAAATGTCCTGTTGCAGC-3′), then cloned by *Bam*HI/*Xba*I digestion into conditional vector pHY304. The resulting plasmid was transformed into the 5448 and 5448AP strains by means of electroporation, and erythromycin-resistant transformants were grown at the permissive temperature for plasmid replication (30°C). Single-crossover chromosomal insertions were selected by shifting to the nonpermissive temperature (37°C), which maintained erythromycin selection [26]. Integrational knockouts were confirmed unambiguously by means of polymerase chain reaction and were designated 5448Δ*hasA* and 5448APΔ*hasA*.

Epithelial cell adherence assays. Assays were performed using HEp-2 cells (human laryngeal epithelial cells) and HaCaT cells (human keratinocyte cells) as described elsewhere [27]. Cells were plated at an inoculum of 2×10^5 cells/well and grown overnight at 37°C in 5% carbon dioxide. Midlogarthmic growth phase GAS were resuspended in Roswell Park Memorial Institute (RPMI) medium plus 2% fetal calf serum and added at a multiplicity of infection of 10:1. Plates were centrifuged for 10 min at 500 *g* and incubated for 30 min at 37°C in 5% carbon dioxide, then washed 5 times with phosphate-buffered saline (PBS) to remove nonadherent bacteria. One hundred microliters of trypsin was added to release cells, which were lysed with 0.02% Triton X-100. Bacteria were serially diluted and plated on THA for enumeration. Bacterial adherence was calculated as a percentage of the initial inoculum. More than 95% cell viability of HEp-2 and HaCaT cells was documented in all assays, as determined by means of trypan blue staining. Bacterial strains grew equally in RPMI medium plus 2% fetal calf serum for the 30-min duration of the experiment. Statistical significance was determined using 1-way ANOVA with the Tukey post hoc test.

Competition adherence assays were performed identically, but with the addition of 2×10^6 colony-forming units (CFUs) per well of an equal mix of the 5448 and 5448AP strains or an equal mix of the 5448Δ*hasA* and 5448APΔ*hasA* strains to cell monolayers. After serial dilutions were plated on THA overnight, 50 individual colonies from each condition (5448 and 5448AP strains or 5448Δ*hasA* and 5448APΔ*hasA* strains) were selected. The proportion of the 5448 strain to the 5448AP strain was determined by the proportion of SpeB-positive colonies to SpeB-negative colonies, respectively, by means of methods that are detailed elsewhere [28]. Assays were performed in triplicate,

and statistical significance was determined using an unpaired *t* test.

Hyaluronic acid capsule assay. Bacterial cultures were grown to midlogarithmic phase in THB. Five milliliters of culture (OD_{600}, 0.4) was centrifuged and resuspended in 500 μL of deionized water. Serial dilutions of bacterial suspension were plated to confirm the equivalent number of CFUs. Four hundred microliters of the bacterial suspension was placed in a 2-mL screw-cap tube with 1 mL of chloroform. Tubes were shaken for 5 min in a Mini-BeadBeater-8 (Biospec Products), then centrifuged at ~13,000 *g* for 10 min. The level of hyaluronic acid in aqueous phase was determined using a hyaluronic acid test kit (Corgenix) according to the manufacturer's instructions.

Fibronectin-binding assays. Fibronectin was bound to 96-well plates (Costar) as described elsewhere [29]. Bacteria were grown to midlogarithmic phase, washed in PBS, and resuspended to a concentration of 2×10^8 CFUs/mL. Plates were washed 3 times with sterile PBS, and 100 μL (2×10^7 CFUs) of bacterial solution was added to each well. Plates were centrifuged at 500 *g* for 10 min, incubated at 37°C for 1 h, then washed 5 times with PBS to remove nonadherent bacteria. Adherent bacteria were released by use of 100 μL of 0.25% trypsin/1 mmol/L ethylenediaminetetraacetic acid (Gibco) for 10 min at 37°C. Bacteria were serially diluted in PBS and plated onto THA for enumeration of CFUs. Bacterial adherence was calculated as a percentage of the initial inoculum. Assays were performed in triplicate, and statistical significance was determined using 1-way ANOVA with the Tukey post hoc test.

Fluorescence microscopy. Glass coverslips were coated with fibronectin by incubating them overnight at 4°C in a 50 μg/mL solution in PBS. Slides were then washed with PBS and blocked overnight at 4°C with PBS plus 1% bovine serum albumin. Bacteria were grown to midlogarithmic phase (OD_{600}, 0.4), centrifuged, and resuspended in PBS to a value of OD_{600} of 1.0. Fluorescein isothiocyanate (FITC) was added to a final concentration of 100 μg/mL and incubated on ice for 30 min. FITC-labeled bacteria were pelleted, washed twice with sterile PBS, and then resuspended to a value of OD_{600} of 0.4 in PBS. Five hundred microliters of FITC-labeled bacterial solution was added to glass coverslips in the bottom of 24-well tissue culture plates. Plates were centrifuged for 10 min at 500 *g*, then incubated for 1 h at 37°C. Coverslips were washed 5 times with PBS, fixed with 4% paraformaldehyde overnight at 4°C, washed again, and mounted on microscopes slides with ProLong Gold (Invitrogen). Slides were visualized using a DeltaVision RT Deconvolution microscope (University of California, San Diego, Neuroscience Microscopy Shared Facility).

Static biofilm formation on polystyrene. Determination of biofilm formation on polystyrene was performed using a modified O'Toole-Kolter crystal violet stain assay [30]. Briefly, 8 individual wells of a black-sided, clear-bottomed, 96-well microtiter plate (Greiner Cellstar; catalog no. 655090) were inoculated with 150 μL of overnight culture diluted 1:100 in THB supplemented with 1% (weight per volume) yeast extract for each strain studied. Plates were sealed with Aeraseal breathable film (Excel Scientific) and incubated for 24 h at 37°C. Plates were washed, and cells were fixed with 4% paraformaldehyde. Six wells were stained with 0.2% crystal violet, extracted in acetone and ethanol, and assayed for crystal violet absorbance at 595 nm for biofilm biomass quantification. The remaining 2 wells for each strain were stained with SYTO 9 nucleic acid stain (Invitrogen), and biofilms were visualized using a Nikon A1 laser scanning confocal microscope. Images were reconstructed from Z sections and rendered for 3-dimensional visualization by use of NIS-Elements software (version 3.0; Nikon). The assay was performed 4 times, and statistical significance was determined using 1-way ANOVA with the Tukey post hoc test.

Static biofilm formation on epithelial cells. The visualization of biofilm formation by GAS strains on epithelial cells was modified from the method of Manetti et al [31]. HaCaT keratinocytes were seeded in RPMI medium into 35-mm tissue culture dishes with a 10-mm diameter glass coverslip insert (Fluorodish; World Precision Instruments) and cultured for 48 h. HaCaT cells were then washed, and 200 μL of 1:10 dilutions of overnight cultures of GAS strains in RPMI medium were added to each dish. After 15 min, HaCaT cells were washed to remove unattached bacteria. Pilot experiments revealed that 8-h incubation was sufficient for wild-type GAS (5448) to form a robust biofilm on HaCaT cells without extensive cell loss and/or death. After 8 h, dishes were fixed with 4% paraformaldehyde, blocked, and blotted with mouse anti–GAS-M1 polyclonal antiserum (provided by Anna Henningham, University of Wollongong, Wollongong, NSW, Australia) and Alexa Fluor 488–conjugated goat antimouse antibody (Invitrogen) as a secondary antibody to allow fluorescent visualization. The HaCaT cells were stained with 4′,6-diamidino-2–phenylindole (nucleic acid stain) and Alexa Fluor 647–conjugated phalloidin (actin stain). The cells were mounted in glycerol, imaged using a Nikon A1 laser scanning confocal microscope, and rendered 3-dimensionally as described above.

Murine skin adherence assay. Bacterial cultures were grown to midlogarithmic phase (OD_{600}, 0.4) and washed with sterile PBS. Bacteria were diluted to 2×10^7 CFUs/mL. Ten microliters of bacterial solution (2×10^5 CFUs) was spotted onto prewarmed THA plates. Once the droplets had dried, agar disks containing the bacteria were excised using an 8-mm biopsy punch. Shaved CD1 mice were anaesthetized with ketamine and xylazine, and bacterial agar disks were affixed with Tegaderm transparent wound dressing (3M). A total of 4 mice, each with 2 disks of the wild-type 5448 bacteria on their left flank and 2 disks of the *covS*-mutant 5448AP bacteria on their

right flank, were used. After 1 h, the mice were euthanized with isoflurane. The skin under the bacterial disks was excised and placed into 2-mL screw-cap tubes containing 1 mL of PBS. The tubes were shaken in a Mini-BeadBeater-8 (Biospec Products) on mix setting for 2 min to remove nonadherent bacteria. Skin was then transferred to a fresh screw-cap tube containing PBS, shaken for 2 min, and transferred to a fresh 2-mL tube containing 1 mL of PBS and 1-mm silica-zirconia beads (Biospec Products). Tissue was homogenized by shaking twice with the Mini-BeadBeater-8 at full for speed for 1 min, with placement on ice between shakings. The homogenate was serially diluted in sterile PBS and plated on THA for enumeration. Bacterial adherence was calculated as a percentage of the initial inoculum. Statistical significance was determined using an unpaired *t* test.

Histological analysis. The in vivo adherence assay was performed as described above using 2×10^7 CFUs/spot. Excised skin was placed in Formalde-Fresh solution (Fisher) overnight, then sectioned and Gram stained at the University of California, San Diego, Histopathology Core Facility (Nissi Varki, director).

LL-37 resistance assays. Bacteria were grown to mid-logarithmic phase and resuspended in PBS plus 20% THB at 1×10^5 CFUs/mL. Ninety microliters of bacteria was then added to 10 μL of varying concentrations of human cathelicidin LL-37 or the murine cathelicidin CRAMP in a 96-well plate.

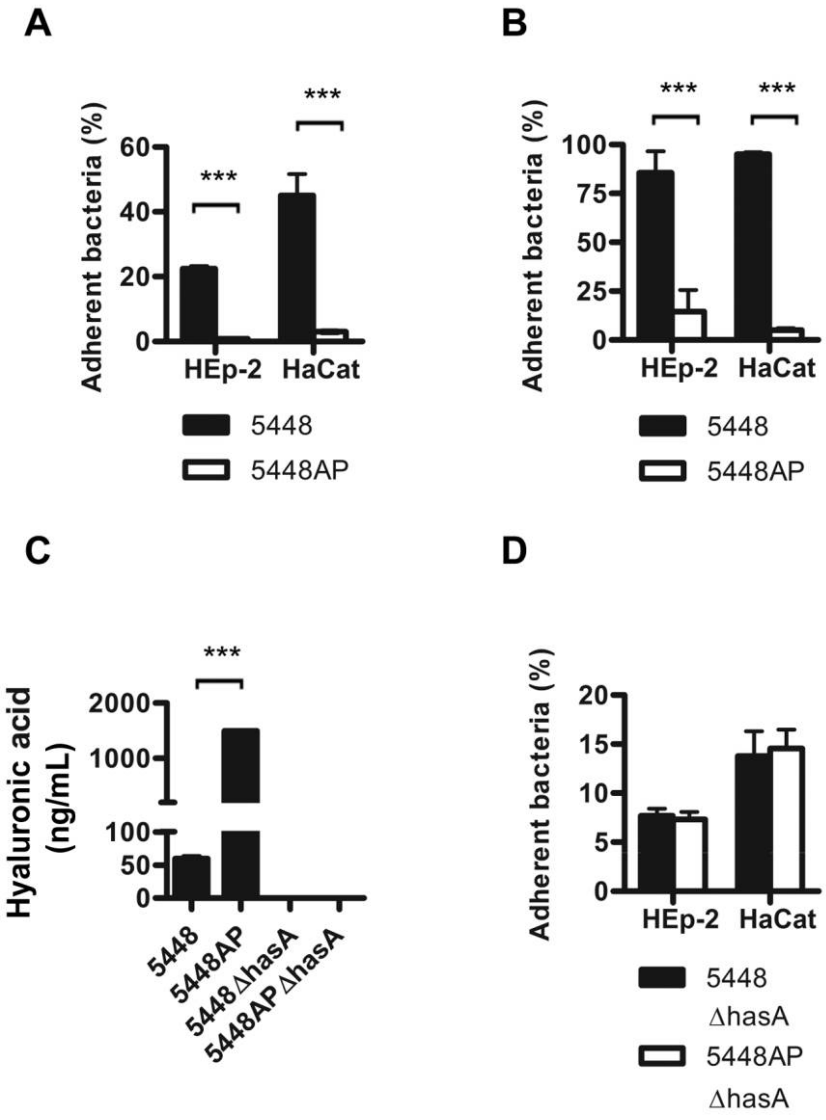

Figure 1. Increased capsule expression and reduced capacity to adhere to epithelial cells as a result of the *covS* mutation in group A *Streptococcus*. *A,* Adherence to HEp-2 cells (human pharyngeal epithelial cells) and HaCaT cells (human keratinocytes) of clinical isolate 5448 and its mouse-passaged *covS*-mutant derivative 5448AP. *B,* Competitive adherence to HEp-2 and HaCaT cells. *C,* Hyaluronic acid capsule levels. The strains 5448Δ*hasA* and 5448APΔ*hasA* are capsule-deficient mutant strains. *D,* Adherence of the 5448Δ*hasA* and 5448APΔ*hasA* strains to HEp-2 and HaCaT cells. Values shown in all panels are means ± standard deviations.

After 24 h, 5 μL of suspension from each well was plated on THA and incubated overnight. The minimum inhibitory concentration (MIC) was defined as the lowest concentration of LL-37 or CRAMP that yielded no detectable bacterial growth when the sample was plated on THA. For experiments in which there was variance in the MIC between replicates, the values are shown as a range.

Ethics approvals. Permission to obtain human blood samples and undertake animal experiments was obtained from the University of California, San Diego, and University of Wollongong human and animal subject protection committees. Human volunteers provided informed consent before blood samples were obtained.

RESULTS

Reduction of adherence to epithelial cells in hypervirulent* covS-*mutant M1T1 GAS. The well-characterized M1T1 clinical isolate 5448 and the isogenic *covS*-mutant derivative 5448AP were used in this comparative analysis. To investigate the ability of wild-type and *covS*-mutant bacteria to adhere to epithelial cells, we utilized 2 human cell lines: HEp-2 laryngeal cells and HaCaT keratinocytes, which represent the throat and skin focal points of GAS colonization and mucosal infection. The 5448AP strain had a marked decrease in adherence, compared with the 5448 strain ($P < .001$), in both HEp-2 and HaCaT cells (Figure 1*A*). In a competition binding assay, the 5448 strain outperformed the 5448AP strain in adherence to both HEp-2 and HaCaT cells (Figure 1*B*). The observation that the adherence of the 5448AP strain was not rescued by coinfection with the 5448 strain suggests that a cell surface factor, not a secreted factor, was responsible for this defect in epithelial cell binding.

Up-regulation of capsule expression has previously been shown in *covS*-mutant GAS [9, 11]. We hypothesized that this up-regulation of capsule in the 5448AP strain was an important contributor to the phenotype of decreased epithelial cell binding. With the exclusion of differences in growth characteristics that may affect subsequent assays, we showed that the capsule-deficient mutant strains, 5448Δ*hasA* and 5448APΔ*hasA*, exhibited similar growth to their respective parent strains in THB and formed chains of similar length (data not shown). The 5448AP strain was found to have statistically significantly more hyaluronic acid capsule than the 5448 strain, whereas the mutant strains 5448Δ*hasA* and 5448APΔ*hasA* were found to have no capsule (Figure 1*C*). Upon a genetically defined disruption of the capsule biosynthesis gene *hasA*, a difference in adherence between the wild-type strain and the *covS*-mutant strain to either epithelial cell line was no longer observed (Figure 1*D*). Although there was no difference observed between the 5448Δ*hasA* and 5448APΔ*hasA* strains, both of these strains displayed less binding than the wild-type 5448 strain. This find-

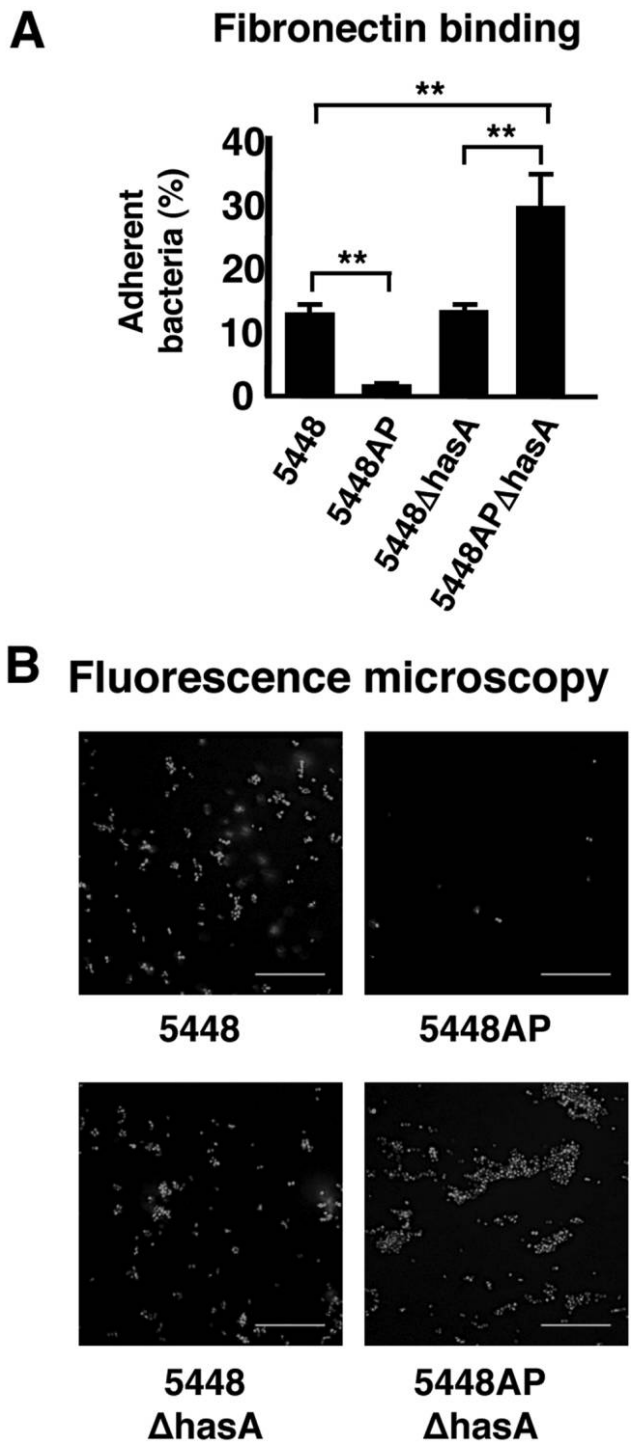

Figure 2. Reduced binding of group A *Streptococcus* (GAS) to fibronectin as a result of the *covS* mutation. *A,* Binding of the 5448 and 5448AP strains and the capsule-deficient mutants 5448Δ*hasA* and 5448APΔ*hasA* to immobilized fibronectin. Values shown are means ± standard deviations. *B,* Fluorescence microscopic analysis of fluorescein isothiocyanate–labeled GAS to fibronectin-coated glass coverslips. *White scale bars,* 20 μm.

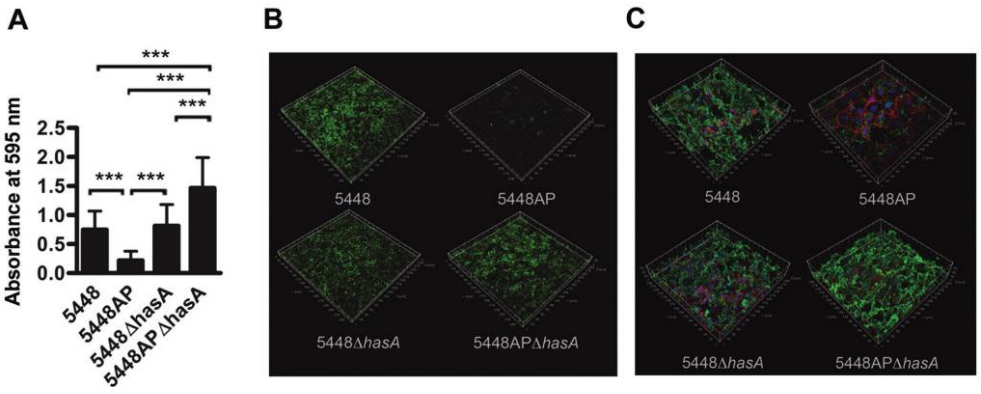

Figure 3. Reduction of biofilm formation of group A *Streptococcus* as a result of the *covS* mutation. *A,* Quantification of biofilm biomass of the 5448 and 5448AP strains and the capsule-deficient mutants 5448Δ*hasA* and 5448APΔ*hasA* after 24 h of growth in 96-well polystyrene microtiter plates. GAS biofilms were stained with crystal violet and extracted with acetone and ethanol. Values shown are means ± standard deviations of absorbance at 595 nm. *B,* Visualization of biofilm formation on polystyrene after 24 h. Biofilms were cultured in 96-well polystyrene microtiter plates and stained with SYTO 9 nucleic acid stain (*green*). Progressive Z sections of the biofilms were imaged at 400× magnification by means of laser scanning confocal microscopy and rendered into 3-dimensional images by use of NIS-Elements software (Nikon). The scale in microns is shown by white grids. *C,* Visualization of biofilm formation on epithelial cells after 8 h. GAS biofilms were cultured on HaCaT human keratinocytes for 8 h, stained, and imaged by means of confocal microscopy. The HaCaT keratinocytes were stained with phalloidin to outline actin (*red*) and the DNA stain 4′,6-diamidino-2–phenylindole to show the nucleus (*blue*). The GAS cells were immunostained with mouse anti–GAS-M1 polyclonal antiserum and Alexa Fluor 488–conjugated goat antimouse secondary antibody (*green*). The scale in microns is shown by white grids.

ing supports a model in which low level capsule expression can contribute to epithelial cell adherence, in particular through hyaluronic acid binding to host CD44 receptors [32, 33], whereas marked hyperencapsulation impairs adherence, likely through cloaking of higher-affinity GAS adhesins and extracellular matrix binding proteins. It is important to note that the M1T1 genome sequence [34] lacks most of the well-characterized GAS surface proteins known to bind fibronectin or other extracellular matrix proteins, including Sfb1, PrtF, PrtFII, SOF, and SfbX. The 2 known GAS fibronectin-binding proteins encoded in the GAS genome sequence (FBP54 and FbaA) are not differentially regulated upon the in vivo selection of the *covS* mutation [9]. Thus, the relative contribution of capsule to adherence in the *covR/S*-intact wild-type M1T1 strain may be greater than in other serotype backgrounds. Nevertheless, our data suggest that up-regulation of capsule expression following *covS* mutation is the principal reason for the reduced binding to epithelial cells that was observed in the 5448AP strain.

Reduced capacity of hypervirulent* covS*-mutant M1T1 GAS to bind fibronectin. Fibronectin is an important component of the extracellular matrix that acts as a target for GAS adhesins; thus, fibronectin binding represents an important initial step in the colonization process [35, 36]. The *covS*-mutant strain 5448AP has a statistically significantly reduced capacity to bind fibronectin ($P < .01$), compared with the wild-type parental strain (Figure 2*A*). The capsule-deficient strain 5448Δ*hasA* exhibited similar binding capacity to the wild-type 5448 strain, whereas strain 5448APΔ*hasA* showed increased binding compared with the 5448AP strain (Figure 2*A*). Fluorescence microscopic analysis of FITC-labeled bacteria corroborated these findings (Figure 2*B*). Reduced capacity to bind extracellular matrix components may affect the ability of *covS*-mutant GAS to colonize the host. Moreover, increased binding by the 5448APΔ*hasA* strain compared with the wild-type 5448 strain suggests that the dramatic capsule up-regulation effectively masks binding increases that would otherwise result from gene-expression changes that are linked to the *covS* mutation.

Reduction of biofilm formation in hypervirulent* covS*-mutant M1T1 GAS. Biofilm formation has been proposed to play a role in GAS colonization, as well as in the persistence and recurrence of GAS infection [31, 37]. We found that the *covS*-mutant 5448AP strain exhibits statistically significantly less biofilm formation than the wild-type 5448 strain ($P < .001$) (Figure 3*A*). The 5448Δ*hasA* strain exhibited similar biofilm formation to the wild-type strain, whereas the 5448APΔ*hasA* strain produced greater biofilms than either the wild-type or 5448Δ*hasA* strains. Taken together, these data illustrate that although further gene regulation differences may affect biofilms, capsule up-regulation in *covS*-mutant GAS is the major factor that limits biofilm formation and effectively negates any potential positive contribution of up-regulated genes in the *covS*-mutant strain. Confocal microscopy was used to visualize biofilm formation on both polystyrene (Figure 3*B*) and epithelial cell layers (Figure 3*C*). Impaired biofilm formation may contribute to a reduced ability of *covS*-mutant M1T1 GAS to colonize and persist in new hosts.

Reduced capacity of hypervirulent* covS*-mutant M1T1 GAS to bind murine skin. A mouse model of skin colonization was used to investigate the comparative capacity of the 5448 and 5448AP strains to colonize the host at a relevant infection site. The *covS*-mutant 5448AP strain was found to have a statistically significantly reduced ability to adhere to live mouse skin, compared with the 5448 strain ($P < .001$) (Figure 4*A*), as further illustrated by the lack of adherent bacteria visible in Gram-stained skin sections (Figure 4*B*). Reduced survival of GAS on live skin may relate to sensitivity to cathelidicin antimicrobial peptides [38, 39]. However, no statistically significant difference between the wild-type strain 5448 and the *covS*-mutant strain 5448AP was noted in resistance to killing by the human cathelicidin LL-37 (MIC for both strains, 14–16 μmol/L) or the murine cathelicidin CRAMP (MIC for both strains, 4 μmol/L). Thus, the colonization defect of the *covS*-mutant strain is likely related to reduced adherence and/or biofilm phenotypes and not increased susceptibility to these cutaneous antimicrobials.

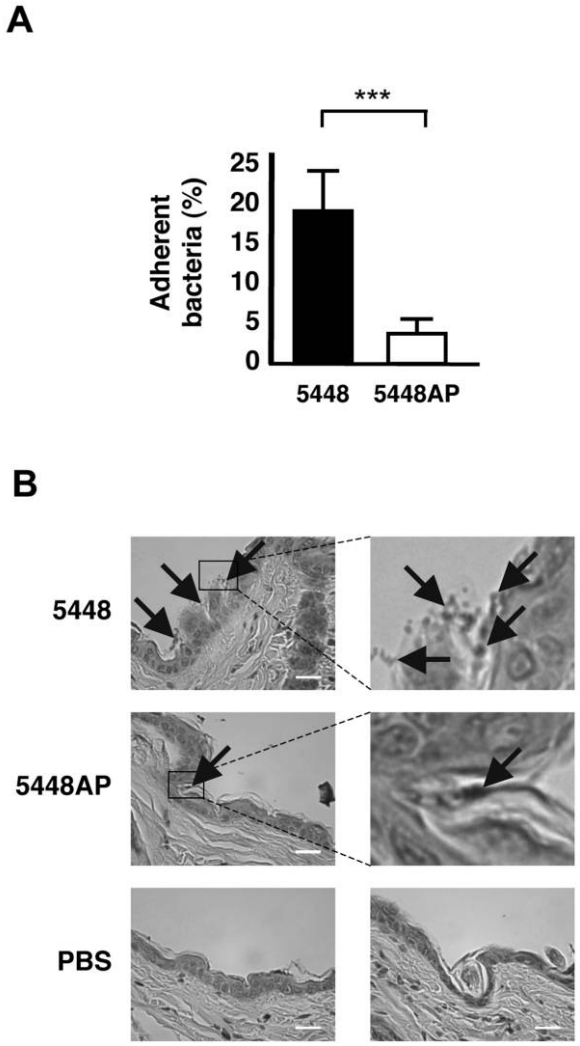

Figure 4. Reduced colonization capacity of group A *Streptococcus* (GAS) as a result of the *covS* mutation. *A*, Adherence of clinical isolate 5448 and its mouse-passaged *covS*-mutant derivative 5448AP to live mouse flank after 1 h of incubation. Values shown are means ± standard deviations. *B*, Gram-stained sections of GAS-colonized skin tissue. *Arrows*, groups of Gram-stained bacteria. *White scale bars*, 50 μm. PBS, phosphate-buffered saline.

DISCUSSION

M1T1 GAS is the most common cause of streptococcal infections in several Western countries [1, 5, 6]. An inverse relationship between SpeB expression in clinical isolates of the M1T1 strain and disease severity indicates that inactivation of SpeB through mutation in the *covR/S* regulator facilitates invasive disease initiation [8–10]. Although the *covS* mutation in M1T1 GAS results in improved neutrophil resistance and propensity for bacterial dissemination [9, 10], here we identify potential counterbalancing fitness costs associated with the *covS* mutation in the realm of GAS fibronectin binding, epithelial adherence, and biofilm formation.

We recovered statistically significantly more of the 5448 strain than we did of the 5448AP strain from the mouse skin adherence model, which shows that the *covS* mutation and its associated phenotypes, in particular up-regulation of capsule biosynthesis, confer a colonization defect in M1T1 GAS despite the dramatic increase in virulence at subsequent stages of infection. These data are supported by a recently published finding of an inverse correlation between the ability to adhere to host cells and GAS virulence [40]. Recently, it was also shown that wild-type GAS outcompete *covS*-mutant strains in human saliva [41]—a finding that supports a model in which such mutations result in increased systemic virulence but come at a fitness cost for other stages of the infection process.

Differential optimization of GAS phenotypic characteristics for survival at different stages of disease pathogenesis is evident in this study. Epithelial cell binding via the extracellular matrix and biofilm formation can promote GAS colonization of the pharynx or skin in the face of competition from the normal resident microflora. However, such close interactions with host cells could be disadvantageous in systemic or bloodstream infection, in which phagocytes of the innate immune system seek to eradicate the pathogen. Hence, there is selective pressure for mutations in *covR/S* with up-regulation of capsule and other neutrophil and serum resistance factors, including SpyCEP [42], streptolysin O [43], Sda1 [9, 10], and streptococcal inhibitor of complement [44]. Analogous patterns of in vivo evolution have been recently described in relation to persistent *Pseudomonas aeruginosa* infection in patients with cystic fibrosis, with positive selection of mutations allowing for genetic changes that are advantageous to life within the host [45].

The global dissemination and persistence over decades of the

M1T1 GAS clone as the prevalent disease-associated strain not only indicates robust colonization properties but also the propensity to mutate to an immunoresistant phenotype that is capable of systemic dissemination. Our data indicate that this phenotype does not become fixed, because the cost of the *covS* mutation, and in particular hyperencapsulation, makes the mutant strain less capable of epithelial colonization than the parent phenotype. It is conceivable that similar paradigms exist for many leading human bacterial pathogens, for which relatively uncommon invasive disease events occur in certain individuals against a much larger backdrop of asymptomatic colonization or self-limited mucosal infection.

Acknowledgment

We thank Anna Cogen (University of California, San Diego) for experimental advice and Anna Henningham (University of Wollongong) for providing antiserum.

References

1. Carapetis JR, Steer AC, Mulholland EK, Weber M. The global burden of group A streptococcal diseases. Lancet Infect Dis **2005**; 5:685–694.
2. Aziz RK, Kotb M. Rise and persistence of global M1T1 clone of *Streptococcus pyogenes*. Emerg Infect Dis **2008**; 14:1511–1517.
3. Chatellier S, Ihendyane N, Kansal RG, et al. Genetic relatedness and superantigen expression in group A streptococcus serotype M1 isolates from patients with severe and nonsevere invasive diseases. Infect Immun **2000**; 68:3523–3534.
4. Tart AH, Walker MJ, Musser JM. New understanding of the group A *Streptococcus* pathogenesis cycle. Trends Microbiol **2007**; 15:318–325.
5. Cleary PP, Kaplan EL, Handley JP, et al. Clonal basis for resurgence of serious *Streptococcus pyogenes* disease in the 1980s. Lancet **1992**; 339: 518–521.
6. Demers B, Simor AE, Vellend H, et al. Severe invasive group A streptococcal infections in Ontario, Canada: 1987–1991. Clin Infect Dis **1993**; 16:792–800.
7. Walker MJ, McArthur JD, McKay F, Ranson M. Is plasminogen deployed as a *Streptococcus pyogenes* virulence factor? Trends Microbiol **2005**; 13:308–313.
8. Kansal RG, McGeer A, Low DE, Norrby-Teglund A, Kotb M. Inverse relation between disease severity and expression of the streptococcal cysteine protease, SpeB, among clonal M1T1 isolates recovered from invasive group A streptococcal infection cases. Infect Immun **2000**; 68: 6362–6369.
9. Sumby P, Whitney AR, Graviss EA, DeLeo FR, Musser JM. Genome-wide analysis of group A streptococci reveals a mutation that modulates global phenotype and disease specificity. PLoS Pathog **2006**; 2:e5.
10. Walker MJ, Hollands A, Sanderson-Smith ML, et al. DNase Sda1 provides selection pressure for a switch to invasive group A streptococcal infection. Nat Med **2007**; 13:981–985.
11. Engleberg NC, Heath A, Miller A, Rivera C, DiRita VJ. Spontaneous mutations in the CsrRS two-component regulatory system of *Streptococcus pyogenes* result in enhanced virulence in a murine model of skin and soft tissue infection. J Infect Dis **2001**; 183:1043–1054.
12. Raeder R, Harokopakis E, Hollingshead S, Boyle MD. Absence of SpeB production in virulent large capsular forms of group A streptococcal strain 64. Infect Immun **2000**; 68:744–751.
13. Musser JM, Stockbauer K, Kapur V, Rudgers GW. Substitution of cysteine 192 in a highly conserved *Streptococcus pyogenes* extracellular cysteine protease (interleukin 1β convertase) alters proteolytic activity and ablates zymogen processing. Infect Immun **1996**; 64:1913–1917.
14. Cunningham MW. Pathogenesis of group A streptococcal infections. Clin Microbiol Rev **2000**; 13:470–511.
15. Hynes W. Virulence factors of the group A streptococci and genes that regulate their expression. Front Biosci **2004**; 9:3399–3433.
16. Nyberg P, Rasmussen M, Von Pawel-Rammingen U, Bjorck L. SpeB modulates fibronectin-dependent internalization of *Streptococcus pyogenes* by efficient proteolysis of cell-wall-anchored protein F1. Microbiology **2004**; 150:1559–1569.
17. Cole JN, Aquilina JA, Hains PG, et al. Role of group A *Streptococcus* HtrA in the maturation of SpeB protease. Proteomics **2007**; 7:4488–4498.
18. Raeder R, Woischnik M, Podbielski A, Boyle MD. A secreted streptococcal cysteine protease can cleave a surface-expressed M1 protein and alter the immunoglobulin binding properties. Res Microbiol **1998**; 149:539–548.
19. Ringdahl U, Svensson HG, Kotarsky H, Gustafsson M, Weineisen M, Sjobring U. A role for the fibrinogen-binding regions of streptococcal M proteins in phagocytosis resistance. Mol Microbiol **2000**; 37:1318–1326.
20. Aziz RK, Pabst MJ, Jeng A, et al. Invasive M1T1 group A *Streptococcus* undergoes a phase-shift in vivo to prevent proteolytic degradation of multiple virulence factors by SpeB. Mol Microbiol **2004**; 51:123–134.
21. Kansal RG, Nizet V, Jeng A, Chuang WJ, Kotb M. Selective modulation of superantigen-induced responses by streptococcal cysteine protease. J Infect Dis **2003**; 187:398–407.
22. Rezcallah MS, Boyle MD, Sledjeski DD. Mouse skin passage of *Streptococcus pyogenes* results in increased streptokinase expression and activity. Microbiology **2004**; 150:365–371.
23. Dalton TL, Scott JR. CovS inactivates CovR and is required for growth under conditions of general stress in *Streptococcus pyogenes*. J Bacteriol **2004**; 186:3928–3937.
24. Cole JN, McArthur JD, McKay FC, et al. Trigger for group A streptococcal M1T1 invasive disease. FASEB J **2006**; 20:1745–1747.
25. Kansal RG, Datta V, Aziz RK, Abdeltawab NF, Rowe S, Kotb M. Dissection of the molecular basis for hypervirulence of an in vivo–selected phenotype of the widely disseminated M1T1 strain of group A *Streptococcus* bacteria. J Infect Dis **2010**; 201:855–865.
26. Nizet V, Beall B, Bast DJ, et al. Genetic locus for streptolysin S production by group A streptococcus. Infect Immun **2000**; 68:4245–4254.
27. Timmer AM, Kristian SA, Datta V, et al. Serum opacity factor promotes group A streptococcal epithelial cell invasion and virulence. Mol Microbiol **2006**; 62:15–25.
28. Collin M, Olsen A. Generation of a mature streptococcal cysteine proteinase is dependent on cell wall-anchored M1 protein. Mol Microbiol **2000**; 36:1306–1318.
29. Jeng A, Sakota V, Li Z, Datta V, Beall B, Nizet V. Molecular genetic analysis of a group A *Streptococcus* operon encoding serum opacity factor and a novel fibronectin-binding protein, SfbX. J Bacteriol **2003**; 185:1208–1217.
30. O'Toole GA, Kolter R. Initiation of biofilm formation in *Pseudomonas fluorescens* WCS365 proceeds via multiple, convergent signalling pathways: a genetic analysis. Mol Microbiol **1998**; 28:449–461.
31. Manetti AG, Zingaretti C, Falugi F, et al. *Streptococcus pyogenes* pili promote pharyngeal cell adhesion and biofilm formation. Mol Microbiol **2007**; 64:968–983.
32. Cywes C, Wessels MR. Group A *Streptococcus* tissue invasion by CD44-mediated cell signalling. Nature **2001**; 414:648–652.
33. Schrager HM, Alberti S, Cywes C, Dougherty GJ, Wessels MR. Hyaluronic acid capsule modulates M protein-mediated adherence and acts as a ligand for attachment of group A *Streptococcus* to CD44 on human keratinocytes. J Clin Invest **1998**; 101:1708–1716.
34. Sumby P, Porcella SF, Madrigal AG, et al. Evolutionary origin and emergence of a highly successful clone of serotype M1 group a *Streptococcus* involved multiple horizontal gene transfer events. J Infect Dis **2005**; 192:771–782.
35. Kreikemeyer B, Klenk M, Podbielski A. The intracellular status of

Streptococcus pyogenes: role of extracellular matrix-binding proteins and their regulation. Int J Med Microbiol **2004**; 294:177–188.
36. Westerlund B, Korhonen TK. Bacterial proteins binding to the mammalian extracellular matrix. Mol Microbiol **1993**; 9:687–694.
37. Lembke C, Podbielski A, Hidalgo-Grass C, Jonas L, Hanski E, Kreikemeyer B. Characterization of biofilm formation by clinically relevant serotypes of group A streptococci. Appl Environ Microbiol **2006**; 72: 2864–2875.
38. Nizet V, Ohtake T, Lauth X, et al. Innate antimicrobial peptide protects the skin from invasive bacterial infection. Nature **2001**; 414:454–457.
39. Zasloff M. Antimicrobial peptides of multicellular organisms. Nature **2002**; 415:389–395.
40. Miyoshi-Akiyama T, Zhao J, Uchiyama T, Yagi J, Kirikae T. Positive correlation between low adhesion of group A *Streptococcus* to mammalian cells and virulence in a mouse model. FEMS Microbiol Lett **2009**; 293:107–114.
41. Trevino J, Perez N, Ramirez-Pena E, et al. CovS simultaneously activates and inhibits the CovR-mediated repression of distinct subsets of group A *Streptococcus* virulence factor-encoding genes. Infect Immun **2009**; 77:3141–3149.
42. Zinkernagel AS, Timmer AM, Pence MA, et al. The IL-8 protease SpyCEP/ScpC of group A *Streptococcus* promotes resistance to neutrophil killing. Cell Host Microbe **2008**; 4:170–178.
43. Timmer AM, Timmer JC, Pence MA, et al. Streptolysin O promotes group A *Streptococcus* immune evasion by accelerated macrophage apoptosis. J Biol Chem **2009**; 284:862–871.
44. Akesson P, Sjoholm AG, Bjorck L. Protein SIC, a novel extracellular protein of *Streptococcus pyogenes* interfering with complement function. J Biol Chem **1996**; 271:1081–1088.
45. Smith EE, Buckley DG, Wu Z, et al. Genetic adaptation by *Pseudomonas aeruginosa* to the airways of cystic fibrosis patients. Proc Natl Acad Sci U S A **2006**; 103:8487–8492.